Chemical Engineering Journal 163 (2010) 438–449

Contents lists available at ScienceDirect

Chemical Engineering Journal

journal homepage: www.elsevier.com/locate/cej

Optimal conceptual design of processes with heterogeneous catalytic reactors

Daniel Montolio-Rodriguez[a], Patrick Linke[a,b,*], David Linke[c], Mirko Z. Stijepovic[b]

[a] Center for Process & Information Systems Engineering, University of Surrey, Guildford, Surrey GU2 7XH, UK
[b] Department of Chemical Engineering, Texas A&M University at Qatar, Education City, PO Box 23874, Doha, Qatar
[c] Catalyst Discovery and Reaction Engineering Department, Leibniz-Institut für Katalyse, A.-Einstein-Str. 29a, 18059 Rostock, Germany

ARTICLE INFO

Article history:
Received 26 April 2010
Received in revised form 31 July 2010
Accepted 3 August 2010

Keywords:
Reaction engineering
Process synthesis
Heterogeneous catalysis
Superstructure optimisation
Styrene

ABSTRACT

This paper presents an optimisation-based method for the screening and conceptual design of processes with heterogeneous catalytic reactors. The method follows a multi-level approach to process synthesis to establish performance targets and identify high-performance designs. At each level, process superstructures are optimised to explore performance limits of the system and to guide the understanding of the relationships between individual design features and process performance. This enables the design engineer to explore trade-offs between performance and structural complexity in a coordinated manner. The method leads to a number of potential design candidates that provide the design engineers with insight into the performance gains that can be expected by increasing design complexity. The method has been developed and implemented for heterogeneously catalysed gas-phase reaction systems and is illustrated with an example in styrene production.

1. Introduction

Conceptual design for process systems with chemical reactions remains a challenging task. Despite the significant progress of optimisation-based process synthesis methods, most industrially relevant systems are considerably more complex and cannot readily be addressed with existing approaches. Existing conceptual process synthesis approaches for reaction systems (e.g. [1–7]) and reaction–separation systems [8–11] are generic and allow large numbers of alternative designs to be searched systematically, including various reactive separation options, but exhibit multiple limitations in their ability to address common industrial systems. In particular, the existing approaches struggle to adequately address heterogeneously catalysed gas-phase reaction systems, which are typically described by complex kinetics and where heat management plays a major role in terms of design feasibility and performance. There is need to develop tailored approaches that provide the ability to capture large numbers of process design alternatives whilst incorporating practical process design limitations and the complex kinetic models typically developed to describe heterogeneously catalysed reactions. Existing approaches are generic in nature and have not been tailored to this class of systems.

The development and design of a heterogeneously catalysed chemical process is still largely sequential. Specific design issues such reactor design, separation systems design or energy integration are addressed as separate steps, one at a time. The overall success of the design activity is hampered by the lack of systematic support tools to assist scientists and engineers involved in the design processes to identify innovative solutions reliably and quickly in the context of the overall design trade-offs. For instance, for many exothermic or endothermic reaction systems, efficient energy management at the reactor and at the process level will have a strong impact on economic success. It is therefore desirable for such systems to develop a process synthesis approach that can exploit the trade-offs of the entire reaction–separation–energy management system in an integrated fashion.

This paper presents an optimisation-based targeting and design strategy that makes use of an optimisation-based process synthesis approach for the systematic identification of conceptual process designs for heterogeneously catalysed gas-phase reaction processes with the use of process superstructures. Section 2 describes the overall synthesis strategy. The superstructure model developments are explained in Section 3 followed by a description of the adopted optimisation approach. An example in styrene production is presented to illustrate the approach.

2. Background and synthesis strategy

Large numbers of design alternatives are generally possible for reactor–separator–recycle systems. These arise from alternative design decisions in various parts of the process structure. For

* Corresponding author at: Department of Chemical Engineering, Texas A&M University at Qatar, Education City, PO Box 23874, Doha, Qatar.
E-mail address: patrick.linke@qatar.tamu.edu (P. Linke).

1385-8947/$ – see front matter © 2010 Elsevier B.V. All rights reserved.
doi:10.1016/j.cej.2010.08.006

instance, decisions on feeding and recycling policies, the number of reaction zones, sizes and types of units, all give rise to distinct designs with differences in relative performance. The goal of process synthesis approaches is to guide the design engineer towards selection of the best performing designs from the possible alternatives. Thus, a process synthesis approach must be based on a representation capable of capturing the large number of design alternatives. Besides the representation of alternatives, process models need to be deployed to predict the performance and feasibility of the different design alternatives and to enable the identification of optimal settings for the design variables with the help of superstructure optimisation models.

Whilst offering the potential to represent the possible alternative process structures, current superstructure-based process synthesis approaches are generic and do not allow the incorporation of constraints and limitations often observed in heterogeneously catalysed reaction systems. In order to effectively address such systems, a tailored approach is developed that handles reactor-separator process design together with heat integration. The individual elements of the superstructure representations and the optimisation approach are presented in the next section.

The application of superstructure optimisation by searching all possible design alternatives simultaneously in a single run often produces complex designs which are later rendered impractical. Instead, superstructures should be deployed to contribute to knowledge generation. Typically, at the beginning of the process synthesis activity, simple process structures (reference structures) are developed as starting points by drawing on past experiences with similar systems. At this point, very little is known about the opportunities to enhance process performance by advanced or novel process designs. Thus, the purpose of the superstructure optimisation is to help answer a number of key design questions in a structured manner:

- What is the performance of the reference designs?
- What is the best possible design performance (target) that can be achieved for this system, regardless of complexity? How far from this target are the reference designs?
- Which design features are present in high-performance designs? What is their contribution to enhancing design performance?
- How much performance is gained by increasing the complexity of the design?

We propose a multi-level synthesis strategy to develop answers to these questions with the help of superstructure optimisations at each level. The strategy is illustrated in Fig. 1. Optimal searches of reduced and full superstructures are carried in structured steps to facilitate the understanding of the system by the engineer in terms of base case performance, performance targets and performance–complexity relationships. This enables the reliable identification of the potential improvements in process performance along with the additional design features associated. At the conceptual design level, the synthesis approach includes two separate levels with the second level consisting of two synthesis steps:

- Level 1: Establishment of a benchmark through identification of the optimal performance of reference structures. At this level, the superstructures are reduced to maintain connectivity and unit functionality. Only continuous and unit specific design variables are exploited in optimisation.
- Level 2A: Identification of the performance limit (target) of the system. At this level, the full superstructures are searched, allowing all design variables to be exploited in optimisation. For instance, all possible interactions between feed, bypass and recycle streams with multiple reaction zones are allowed to be explored. From the resulting optimal design candidates, the performance limit is obtained and insights into promising process features are obtained from the identified high-performance solutions.
- Level 2B: Identification of relationships between process performance and specific design features and combinations thereof. The superstructure optimisations performed at Level 2A yield high-performance designs typically containing features different from the reference structures. At this level, these features are systematically investigated through the optimisation of reduced superstructures by increasing the search space from simple to complex designs. Starting from the base case structures, the search space is increased by adding the identified potentially beneficial process design features observed at Level 2A. Consequently, the design complexity is increased and the resulting improvement in process performance can be assessed. This stage is iterative and the understanding acquired in each iteration drives the search in subsequent searches. In each iteration, complexity (number of reactive units and/or number of stream connections) is increased and the resulting superstructure is optimised.

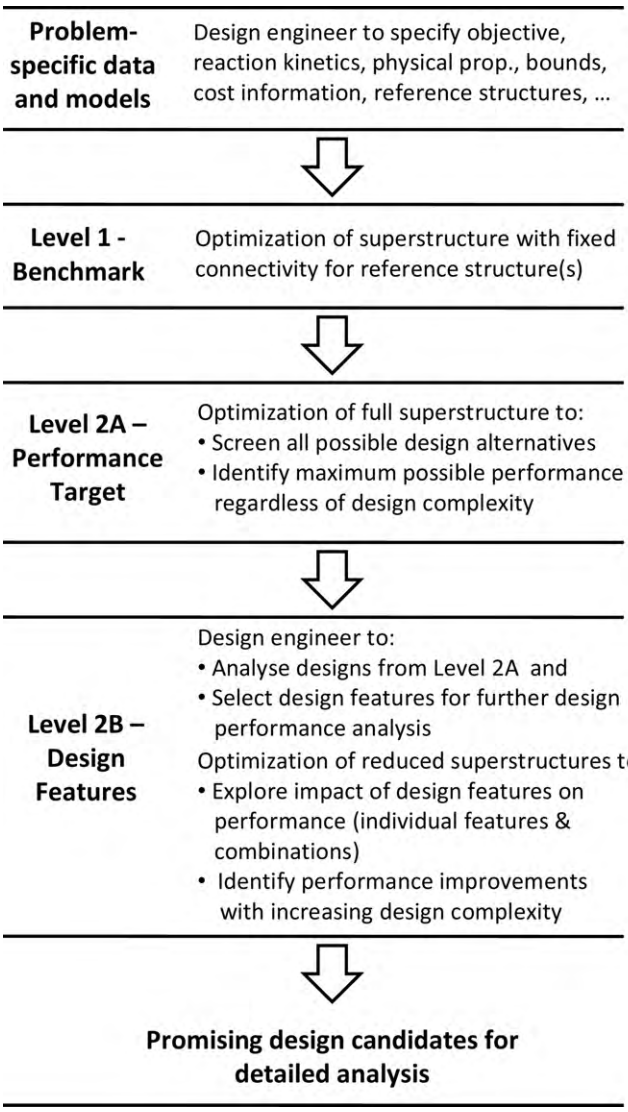

Fig. 1. Multi-level approach for screening and conceptual design.

Level 2B yields design candidates deemed promising by the design engineer in terms of the acceptable balance between per-

formance and structural complexity. Levels 1 and 2 constitute the conceptual design levels of the approach. Additional synthesis levels address the evolution of the identified conceptual designs with the help of more detailed process models. This further evolution of the design is not addressed here and will be presented in a separate publication.

The proposed multi-level synthesis approach employs superstructure optimisation at the various levels of the search. The employed superstructure optimisation framework builds upon previous work by Linke and Kokossis [10,12] which has proven robust in a number of complex applications in bioreaction systems [13,14], reactive and reaction–separation problems [10,15] and a complex case study involving heterogeneously catalysed reactions for acetic acid production [16]. This paper introduces refinements to the superstructure optimisation framework to enable applications involving heterogeneously catalysed reactors. More importantly, it focuses on the application of superstructure optimisation as part of the overall synthesis strategy, i.e. on how the superstructure optimisation framework is applied during the synthesis exercise by systematically extracting design alternatives in a multi-level approach.

3. Synthesis units and network representation

The process synthesis representations build upon the basic synthesis units and superstructure representation introduced by Linke and Kokossis [10]. A superstructure includes several reactor units connected in every possible way through mixers and splitters. Separation units are included to enable reactor–separator–recycle structures. Superstructure representations are customised for heterogeneously catalysed gas-phase reaction systems and adapted to include practical constraints that are observed in practical applications. At the outset of the synthesis exercise in Level 2A, the process structure is unknown and the combinatorial complexity is generally high. The main design decisions that need to be made for heterogeneously catalysed gas-phase reaction systems include reactor design and operation, interactions via recycles between reaction and separation systems, and separation system design and operation. The reaction representations include combinations of generic units that embed options relating to mixing (plug-flow or well-mixed), temperature policies, mass of catalyst and constraints regarding heat management and component concentrations. The energy management constraints for individual reactor units are derived from physical limits that are present in different heterogeneously catalysed reaction system designs. Concentration limits are incorporated as design constraints and can be set with respect to different components to incorporate safety constraints. Separations are represented in aggregated form to decompose the design problem. Energy integration is performed for each solution explored to consistently assess the performance of designs that have been optimised for energy efficiency.

3.1. Reactor unit representation

The models employed for the representation of catalytic reactors are continuously stirred tank reactor (CSTR) and approximation of the pseudo-homogeneous one-dimensional plug-flow reactor (PFR) model. The PFRs are approximated by a series of isothermal equal catalyst load sub-CSTRs as proposed by Kokossis and Floudas [1]. Fixed-bed reactors (FBRs) or multi-tubular reactors (MTRs) can be represented conceptually by this approximation. Non-isothermal effects are incorporated using the temperature profile approach as described in Linke and Kokossis [10]. This approach allows non-isothermal effects to be described without the need to converge energy balances in the simulation of a reactor module. The basic model equations for the CSTR and PFR reactor units as part of the superstructure formulations are presented in Linke and Kokossis [12] and not repeated here.

Theoretically, if catalyst pellets are considered, internal mass transfer limitations inside the pellets can occur. The incorporation of diffusion process models and catalyst pellet design aspects into the reactor synthesis units is presented elsewhere [17] and can be adopted when needed. However, in all applications of the presented method, internal diffusion processes were either lumped into the kinetic expressions or assumed negligible.

The pressure losses for the approximation of the pseudo-homogeneous one-dimensional PFR model without radial temperature profile approximation are considered to follow Ergun [18] equation. The Ergun expression models the pressure losses (P_t) along the length of the reactor (z) as:

$$-\frac{\delta P_t}{\delta z} = f\frac{\rho_g u_0^2}{d_p} \tag{1}$$

where f is the friction factor, ρ_g is the gas density, u_0 is the superficial velocity and d_p is the diameter of the catalyst particle. If the reactor is discretised in segments, the pressure losses can be represented as:

$$\frac{\Delta P_t}{\Delta z} = f\frac{\rho_g u_0^2}{d_p} \tag{2}$$

Ergun proposed the following expression for the friction factor:

$$f = \frac{1-\varepsilon}{\varepsilon}\left[a + \frac{b(1-\varepsilon)}{Re}\right] \quad a = 1.75 \quad b = 150 \tag{3}$$

where ε is the void fraction of the catalyst bed and Re is the Reynolds number. The pressure losses inside the reactors vary depending on the type of reactor. The pressure losses for CSTRs are assumed to be a typical value in early synthesis stages.

Certain constraints are particular to the heterogeneously catalysed gas-phase reaction systems. They can be divided in concentration constraints and temperature and heat transfer constraints. Concentration constraints refer to limits on the amounts of specific components in order to avoid problems such as unsafe scenarios (e.g. high concentrations of oxygen at elevated temperatures) or conditions leading to fast catalyst deactivation (e.g. to low steam-to-reactant ratio). Such concentration limits are directly incorporated in the problem formulation as inequality constraints. Temperature constraints limit the maximum allowable temperature in the system, whereas heat transfer constraints stem from the physical limits of catalytic reactors and are captured by our representation as described in the next paragraphs.

CSTRs operate isothermally with the reactor temperature being a degree of freedom. For reactors with plug-flow, the shape of the imposed temperature profile is optimised. In order to ensure feasibility of the imposed temperature profile, the amount of heat to be exchanged between each reactor ($q_{reactor}$) or section of a reactor (q_{isc}) and the utility media has to be physically achievable. For a given reactor with a given temperature profile, two heat balances are performed to establish feasibility. First, a heat balance is set up for feed and product streams to determine the heat released or added to or from a CSTR or PFR section:

- For a CSTR (reactor):

$$q_{reactor} = \sum_{ic=1}^{ncomp} m_{ic,reactor} h_{ic,reactor}(T_{reactor}) - \sum_{ic=1}^{ncomp} m_{ic,in\_reactor} h_{ic,in\_reactor}(T_{in\_reactor}) \tag{4}$$

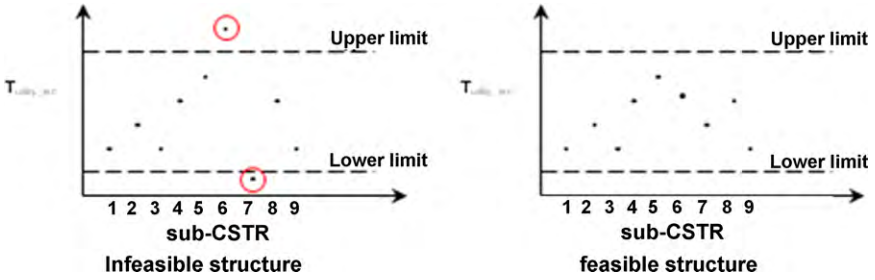

Fig. 2. Heat exchange media temperature profiles for a PFR formed by nine sub-CSTRs that exchanges heat with nine heat exchangers.

- For the first cell of a PFR (isc = 1):

$$q_{isc=1} = \sum_{ic=1}^{ncomp} m_{ic,isc=1} h_{ic,isc=1}(T_{isc=1}) - \sum_{ic=1}^{ncomp} m_{ic,in\_reactor} h_{ic,in\_reactor}(T_{in\_reactor}) \quad (5)$$

- For a subsequent cell a PFR (isc > 1):

$$q_{isc} = \sum_{ic=1}^{ncomp} m_{ic,isc} h_{ic,isc}(T_{isc}) - \sum_{ic=1}^{ncomp} m_{ic,isc-1} h_{ic,isc-1}(T_{isc-1}) \quad (6)$$

where h_{ic} is the enthalpy of each component, m_{ic} is the molar flow of each component, $T_{in\_reactor}$ is the inlet temperature of the reactor, $T_{reactor}$ is the operating temperature of the reactor and T_{isc} is the operating temperature of each section of reactor. Next, the temperature of the utility medium is calculated as:

- For a CSTR (reactor):

$$T_{utility} = T_{reactor} - \frac{q_{reactor}}{UA} \quad (7)$$

- For a cell of a PFR:

$$T_{utility\_isc} = T_{isc} - \frac{q_{isc}}{UA} \quad (8)$$

where U is the overall heat transfer coefficient, A is the heat exchange area, $T_{utility}$ is the temperature of the utility media for a reactor and $T_{utility\_isc}$ is the temperature of the utility media for each section of reactor. If this temperature stays within acceptable limits (Fig. 2), which are directly linked to the reactor types and features, the heat exchange is considered to be feasible. Therefore, a design in which all reaction sections meet this heat exchange constraint is considered a feasible solution in the optimal search. Otherwise, the design is rejected during the optimisation.

For the approximation of a one-dimensional PFR model, the temperature imposition method assumes that the reactor exchanges heat with as many heat exchangers as sub-CSTRs employed for the PFR approximation (Fig. 3). Such a scenario leads to a temperature profile of the utility media that does not follow a progression along the reactor, which can be physically achieved with an independent heat exchanger for each control volume of the reactors (see in Fig. 2 the scattered points of $T_{utility\_isc}$ vs. sub-CSTR). Although this situation can be considered as an ideal case and is impractical from an application viewpoint, it allows narrowing the search space and focussing the efforts on promising regions disregarding the options that even in these ideal circumstances, still require impossible heat exchange scenarios. Other impractical scenarios identified are those in which a single reactor requires heating and cooling. Detailed information on the reactor models employed are presented in Appendix A.

3.2. Separation system representation

The separation units of the superstructures are represented and modelled as sequences of separators in the form of input-output models as described in Linke and Kokossis [12]. The input to each separator determines its output based on component split fractions. The units are associated with cost expressions and developed as follows. In case of grassroots design, the separation-sequencing problems are repeatedly solved using appropriate synthesis techniques for different feeds to develop a separation sequence cost as a function of the feed flow and feed composition. In retrofit cases where the separation equipment shall be kept, the separation trains are either modelled using short-cut models and simulated on the fly. Alternatively similar to the grassroots design case, separation train simulations are repeatedly solved followed by equipment cost estimations for different feeds to develop a separation sequence cost as a function of the feed flow and feed composition.

Since the components present in the reaction section are known and constitute the feed to the separation section, their flow and composition ranges can be estimated to narrow the ranges to be used in developing the cost function.

3.3. Energy integration

Energy management has significant impact on design performance. We therefore energy integrate each design generated during optimisation. The Problem Table Algorithm [19] is used to evaluate maximal heat recovery within system. The external utilities are selected according to the temperature at which they are required and their flows are estimated through heat balances. The Townsend and Linnhoff [20] method is adopted for estimating heat

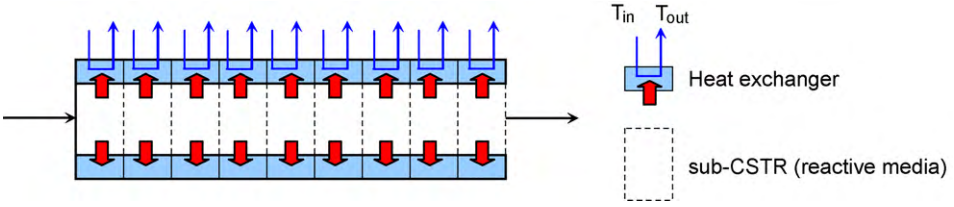

Fig. 3. Cooled PFR represented by nine sub-CSTRs that exchanges heat with nine heat exchangers.

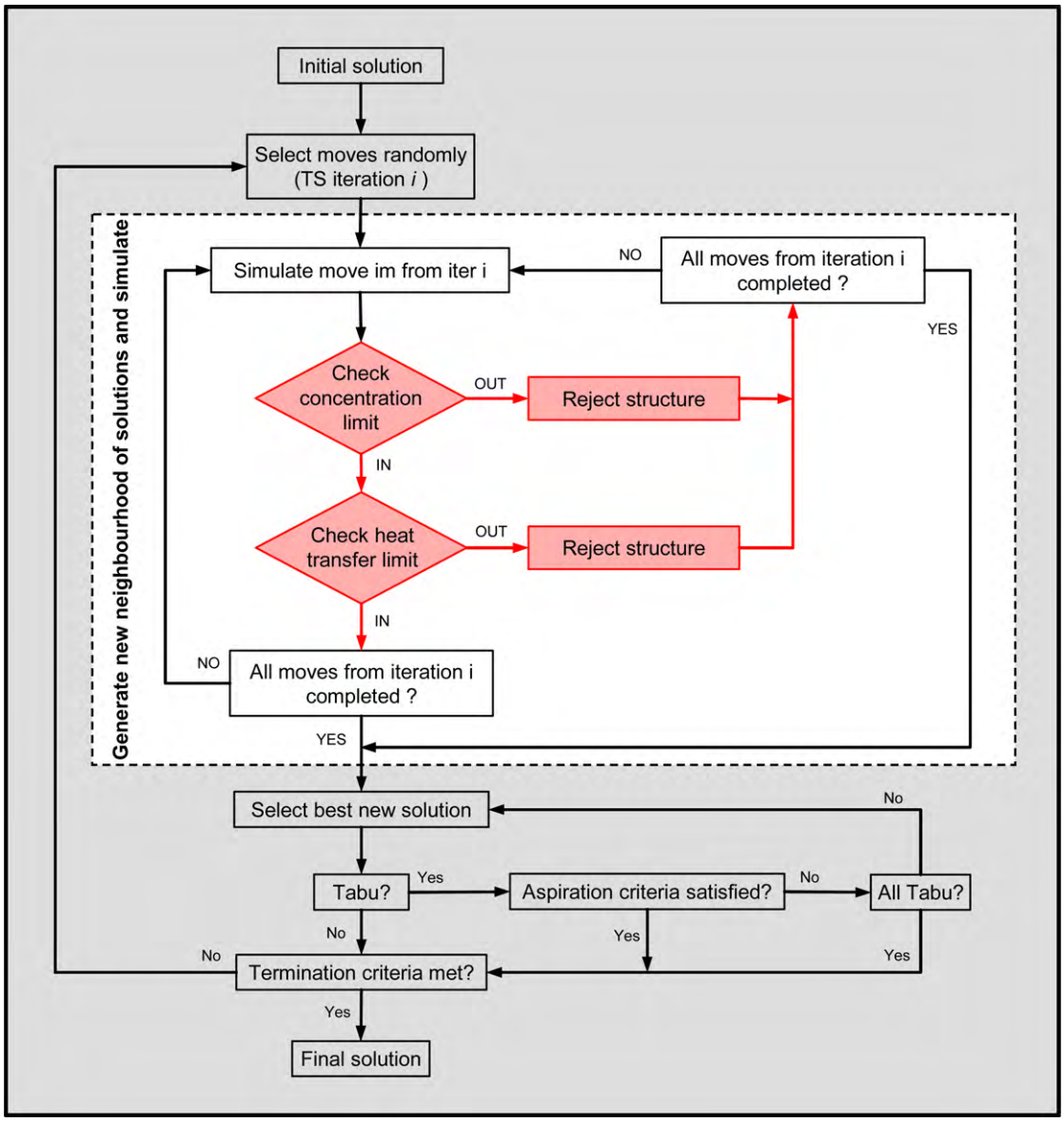

Fig. 4. Implementation of Tabu Search (TS) algorithm.

exchanger area targets. The minimum number of heat exchange units is calculated form equation proposed by Linnhoff et al. [21]. The heat recovery pinch value and position correspond to an economic minimum temperature difference between the energy and the capital costs of the heat exchanger network. The outputs of the energy integration are the heat exchange area, the number of units that form the network and the external utilities required.

4. Network optimisation

The superstructures consisting of reactor and separator units are optimised using the Tabu Search meta-heuristics [10]. The employed objective functions for process designs screening can in principle be any function of variables of the system, i.e. flow rates, compositions, equipment sizes, or energy demand. The default objective function employed in this work is the annual gross profit (AGP). The default AGP takes into account the capital and operational costs of the key equipment items. These are compressors, reactors, reboilers and condensers of distillation columns and the heat exchanger network. The AGP is calculated as:

$$\text{AGP} = \text{product value} - \text{operating cost} - \text{capital cost} \times \text{annualisation factor} \quad (9)$$

where

$$\text{annualisation factor} = i \cdot \frac{(1+i)^{\text{PBP}}}{\left((1+i)^{\text{PBP}} - 1\right)} \quad (10)$$

in which i is the interest rate and PBP the payback period. The network optimisation is performed using Tabu Search [22]. Tabu Search applications have been applied to the synthesis of heat exchanger networks [23], in batch plant process design [24], reactor networks [6] and in reaction–separation and reactive/separation systems [10,12]. Tabu Search algorithm for the multi-level approach is implemented as shown in Fig. 4. A single optimisation study using Tabu Search consists of multiple optimal searches starting from different initial solutions [12].

Tabu Search explores the search space of feasible solutions by performing a series of random moves (alterations on the current state). As a result, moves are associated with the degrees of freedom

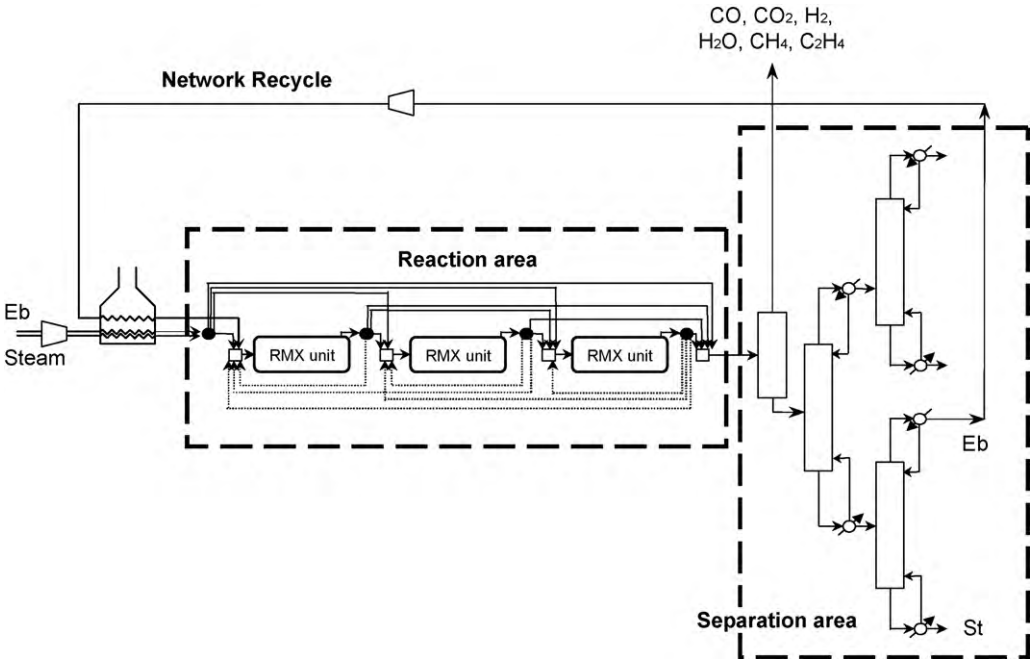

Fig. 5. Superstructure representation for the styrene production process.

of the optimisation. The set of moves considered during superstructure optimisation varies between the different levels of the proposed multi-level synthesis approach. The moves can be classified into moves on continuous design variables (e.g. unit sizes) and discrete design variables (e.g. existence of units and connections). At Level 1, process structures are limited to the reference structures only and very limited discrete options are considered (e.g. tube diameter in a tubular reactor). At Level 2A, the full superstructures are searched and all discrete decisions are considered to enable performance targeting. Then, at Level 2B, the discrete variables are again limited to explore in detail those specific design features that are identified at Level 2A. Thus, the superstructure optimisation problems encountered at Level 2A of the proposed multi-level synthesis strategy are the most complex.

The superstructure optimisation considers the following moves, with the synthesis level at which the moves are considered specified in brackets:

- the addition/removal of generic units (Level 2A),
- the change of type of a generic unit (Level 2A),
- the change in size of a generic unit (Level 1, Level 2A, Level 2B),
- the re-sizing of generic units while keeping the overall network size (Level 1, Level 2A, Level 2B),
- the addition/removal of streams that interconnect generic units including recycles and bypasses (Level 2A – full connectivity, Level 2B – limited connectivity),
- the change of source/sink position of the streams that interconnect generic units (Level 2A – full connectivity, Level 2B – limited connectivity),
- the change in split fractions of streams that interconnect generic units (Level 1, Level 2A, Level 2B),
- changes in temperature profiles for non-isothermal reactors, such as the change of the temperature profile direction (ascending/descending), or the modification of the parameters that define the temperature profile of a generic unit (Level 1, Level 2A, Level 2B),
- the increase/decrease of the operating temperature for isothermal generic units if temperature is a variable for optimisation (Level 1, Level 2A, Level 2B).
- the general increase/decrease of the temperature of all the generic units that form the network (Level 1, Level 2A, Level 2B),
- the decrease/increase of the temperature of all units and the increase/decrease of the size of all the generic units (Level 1, Level 2A, Level 2B),
- the increase/decrease of the size of a generic unit and the decrease/increase of its temperature while increasing/decreasing the temperature of the rest of generic units (Level 1, Level 2A, Level 2B),
- in cases where the amount of a network feed stream is a variable for optimisation (Level 1, Level 2A, Level 2B):
  - the increase/decrease in feed flow rate,
  - the increase/decrease of its amount and the addition/removal of another feed stream bypass,
  - the increase/decrease of its amount and the decrease/increase in the temperature of a generic unit,
  - the increase/decrease of its amount and the decrease/increase in the temperature of all the generic units.
- the increase/decrease of catalyst particles size (Level 1, Level 2A, Level 2B).
- the increase/decrease of reactor diameters. The generic units that represent are considered to be vessels and their diameters are treated as continuous variables (Level 1, Level 2A, Level 2B).
- the increase/decrease of the nominal diameter of tubes inside MTRs. As a default standard, we have considered schedule 40 tubes in this work (Level 1, Level 2A, Level 2B).
- the increase/decrease of the number of reactor tubes (Level 1, Level 2A, Level 2B).
- the increase/decrease of the void fraction of the catalyst bed in FLBRs (Level 1, Level 2A, Level 2B).

The superstructure optimisation framework with its optimisation algorithm (Tabu Search) has been implemented in Fortran using Compaq Visual Fortan Standard Edition 6.6.0 as an extension of the implementation described in Linke and Kokossis [12]. The non-linear systems of equations that define the simulation problem solved for each design instance explored during the optimisation problem are solved using the NEQLU routine by Chen and Stadtherr [25].

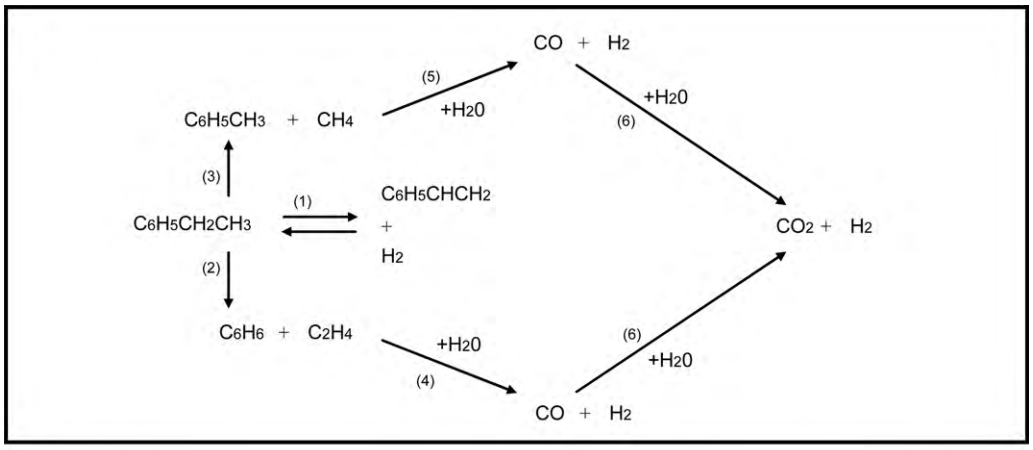

Rate equation	A_i	E_i / R (K)
$^{1}r_1 = k_1\left(p_{ethylbenzene} - p_{styrene}p_{hydrogen}/K_{eb}\right)$	1.51286	10925
$r_2 = k_2 p_{ethylbenzene}$	$5.6197 \times 10^{+5}$	25000
$r_3 = k_3 p_{ethylbenzene} p_{hydrogen}$	1.3446	11000
$r_4 = k_4 p_{steam} p_{ethylene}$	9.3016×10^{-1}	12500
$r_5 = k_5 p_{steam} p_{methane}$	5.3163×10^{-2}	7900
$r_6 = k_6 p_{steam} p_{carbon\_monoxide}\left(P/T^3\right)$	1.6769×10^{9}	8850

Fig. 6. Reaction paths and rate expressions for the styrene production process.

5. Illustrative example

A case study in the production of styrene is used to illustrate the methodology. Styrene can be produced commercially by dehydrogenation of ethylbenzene or via ethylbenzenehydroperoxide. In this work, the gas-phase heterogeneously catalysed dehydrogenation of ethylbenzene [26] is the selected production process. The feed in gaseous state (ethylbenzene with impurities along with steam) is heated before being fed to the reaction units (Fig. 5).

The kinetics for the catalytic dehydrogenation of ethylbenzene to produce styrene (Fig. 6) are taken from the ATHENA Process Simulation Framework case study (Silvaco International, 1994): "Catalytic production of styrene". The kinetic constants follow the Arrhenius expression. For the same kinetic parameters as the ones employed here, Abdalla et al. [27], Elnashaie and Elshishini [28], and Yee et al. [29] have compared the performances obtained with two different reactor models: (1) a pseudo-homogeneous one-dimensional PFR model without radial temperature profile approximation; (2) a more detailed heterogeneous model that takes into account the diffusion in the catalyst pellet. All studies concluded that both models showed very similar performances due to the fact that mass transfer does not limit the reactions in the system. These conclusions were reached for catalyst particles with equal or bigger diameter, than the ones employed here. Therefore, models based on a pseudo-homogeneous PFR model that does not take into account diffusion in the catalyst pellet, can be employed here without experiencing inaccuracies.

The process is optimised given a fixed feed rate of ethylbenzene with impurities of 32,000 ton/yr [30]. The feed composition is presented in Table 1. The amount of the second feed (steam) is determined by the optimisation search. Unreacted and produced components (ethylbenzene, styrene, toluene, benzene, ethylene, methane, steam, carbon monoxide, carbon dioxide and hydrogen) are cooled before entering the condenser. The condenser separates the condensable components (ethylbenzene, styrene, toluene and benzene) from the rest, which are purged. Condensable components are separated in a distillation sequence and benzene, toluene and styrene are the products of the process, whereas unreacted ethylbenzene is recycled to the first reactor. The goal of the study is to identify trends and key features of the system of reactors that enhance the overall process performance in terms of profitability. The problem data for the study is summarised in Appendix B.

5.1. Synthesis procedure: Level 1

The reactor type widely used in industry for the production of styrene by dehydrogenation of ethylbenzene is the adiabatic reactor [26]. The process representations for such reactor have not been integrated in this work as it included as an instance of the non-isothermal PFR. In order to determine the maximum AGP of the typical industrial case, an adiabatic reactor model comprised by mass and energy balances for the one-dimensional PFR cell representation has been included and the process optimised to determine the optimum reactor volume and inlet temperature. The design and operating conditions for the adiabatic reactor are presented in Table 2. The optimal volume identified for this case is the

Table 1
Feed to the styrene production process.

Parameter	Unit	Value
Ethylbenzene (Eb)	kmol/h	36.87
Styrene (St)	kmol/h	0.67
Benzene (Bz)	kmol/h	0.11
Toluene (Tol)	kmol/h	0.88
Steam	kmol/h	To be optimised

Table 2
Design and operating conditions for the adiabatic reactor [30].

Parameter	Unit	Value
Reactor diameter	m	1.95
Catalyst bulk density	kg/m^3	2146
Catalyst particle diameter	m	4.7×10^{-3}
Bed void fraction	–	0.445
Inlet pressure	Bar	2.4

maximum allowable and the optimal inlet temperature is 929 K. Apart from the process with the adiabatic reactor, the other two base cases optimised in this stage include a processes with a single CSTR and a process with a single MTR. The option of exchanging heat with either a heating or cooling media is explored in both cases. The maximum profits identified for three base case processes are presented in Table 3. Both CSTR and MTR are heated using utility. The optimised process with the MTR outperforms the process with an adiabatic reactor by 11%. The optimised process with a CSTR underperforms the process with the adiabatic reactor by 17%.

5.2. Synthesis procedure: Level 2A

In the performance targeting step, the full superstructure (Fig. 5) is optimised without imposing structural constraints, *i.e.* all structural and operational variables are explored such as reactor units addition or deletion, reactor type changes, temperature changes, changes to the bypasses and recycles between reactors and feed distributions. PFRs (FBRs and MTRs) and CSTRs are considered for the optimisation. A total of 30 optimisation experiments are performed. All the experiments start from different initial feasible points. The maximum profit (performance target) identified is 11.37 M$/yr, which represents an 18% improvement with respect to the adiabatic reactor. The analysis of all the experiments shows that:

- Multiple reactors are present in all identified solutions. All the reactors for the cases with higher objective function values are PFRs (MTRs) except for a few cases, where the superstructure consists of a PFR (MTR) followed by a CSTR.
- Ethylbenzene side stream feeding is present in many of the final process design candidates. Superheated steam side stream feeding is not present in any of the final process design candidates.
- Internal recycles between reactors are present in a third of the final process design candidates. Recycle rates are small.

Table 3
Performance of the base case designs for the styrene production process at Level 1.

Structure	Performance[a]	Unit	Value
Adiabatic reactor	AGP	M$/yr	9.66
	CPU time	h	6.65
PFR (MTR)	AGP	M$/yr	10.73
	CPU time	h	0.93
CSTR	AGP	M$/yr	8.05
	CPU time	h	0.15

[a] AGP results are taken from the best cases out of ten converged optimisation runs. CPU times (Intel XEON 2.0 GHz processor) are average values.

Table 4
Performance of the optimised designs for the styrene production process at Level 2B.

Structure	Performance[a]	Unit	Value
PFR (MTR) + CSTR	AGP	M$/yr	11.13
	CPU time	h	2.87
PFR + PFR (MTRs)	AGP	M$/yr	11.36
	CPU time	h	7.05
PFR + PFR + PFR (MTRs)	AGP	M$/yr	11.37
	CPU time	h	12.47

[a] AGP results are taken from the best cases out of ten converged optimisation runs. CPU times (Intel XEON 2.0 GHz processor) are average values.

- Bypasses are present in almost none of the final process design candidates.

5.3. Synthesis procedure: Level 2B

Targeted structures based on the analysis of results from the previous structures are investigated. Two structural limitations are imposed: No reactor units can be added or deleted during the optimal search and no bypasses and recycles between reactors are allowed. However, feed bypasses to the reactors are possible. The three cases explored include the reactor combinations PFR followed by CSTR as well as two and three PFRs connected in series. The analysis of these designs shows that for the structure formed by a PFR and a CSTR, the volume of the CSTR is minimised. Therefore, its influence on the profit is small. The main reason for the improvement in profit over the design with a single PFR (Table 3) stems from the fact that 0.5 M$/yr is saved in superheated steam due to the ethylbenzene side stream feeding identified. The two structures that consist of series of PFRs, in which there is also ethylbenzene side stream feeding, produce very similar results. For two PFRs in series, the AGP improves with respect to the single PFR by 5.9% whereas for the three PFRs in series, it is improved by 6.0% (Table 4) and reaches the maximum objective identified in the targeting stage.

In order to comprehend the difference in performances between the processes with one and three PFRs, the results for both cases are compared. The benefit/detriment in Tables 5–7 is of the three PFRs structure with respect to the one PFR structure. For both cases, the results of the solutions with the best AGPs are presented. The analysis of results shows that the ethylbenzene side feeding identified for the three PFRs structure results in a flatter steam profile inside the reactors (steam over reactant (SOR) at the inlet of the three PFRs in series is at its lower bound), which increases the ethylbenzene conversion, the toluene and the benzene selectivity and reduces the styrene selectivity (Table 7). This reduces the product revenues by 0.40 M$/yr through reductions in styrene revenues by 0.61 M$/yr which are partly offset by increases in benzene and toluene revenues. However, these lost revenues are outweighed by reductions in steam feed requirements. The process with three PFRs in series saves 0.70 $M/yr in steam, 0.16 M$/yr in its compression and requires a smaller feed compressor (annualised value of 0.11 M$/yr) as compared to the process with a single PFR. In addition, the higher conversion of ethylbenzene for three PFRs in series results in a lower amount of ethylbenzene recycled from the distil-

Table 5
Capital costs for styrene production process designs.

Structure	Units	External compressor	Feed compressor	Reactor	Heat exchanger network
One PFR (MTR) structure	M$	0.30	1.04	0.22	1.75
Three PFRs (MTRs) structure	M$	0.25	0.75	0.32	1.65
Benefit (+)/detriment (−)	M$	+0.05	+0.29	−0.10	+0.10
Annualised benefit/detriment	M$/yr	+0.018	+0.108	−0.038	+0.037

Table 6
Product values and operational costs (M$/yr) for styrene production process designs.

Structure	Product value	Raw material	External compression	Feed compression	Reactor heating
One PFR (MTR) structure	29.17	16.11	0.11	0.47	0.52
Three PFRs (MTRs) structure	28.77	15.42	0.08	0.32	0.47
Benefit (+)/detriment (−)	−0.40	+0.70	+0.03	+0.15	+0.05

Table 7
Selectivities (%), conversion (%) and SOR[a] for styrene production process designs.

Structure	Styrene selectivity	Benzene selectivity	Toluene selectivity	Ethylbenzene conversion	SOR reactor inlet	SOR reactor outlet
One PFR (MTR) structure	92.56	2.77	4.35	98.97	7.0	11.0
Three PFRs (MTRs) structure	90.28	3.10	6.30	99.17	7.0, 7.1 and 7.0	8.9, 8.3 and 8.8

[a] SOR is the molar ratio of steam over reactant (see Appendix B).

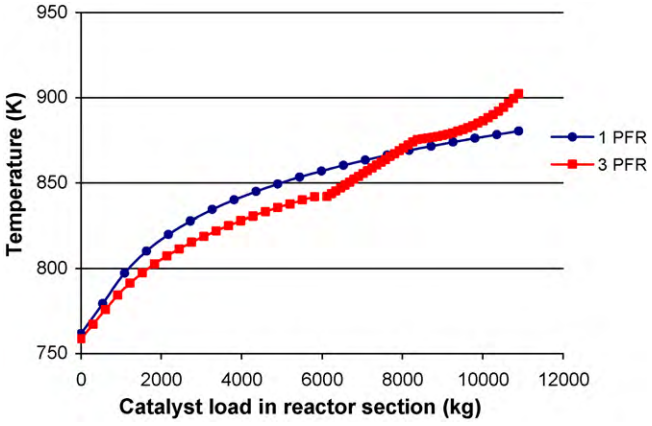

Fig. 7. Temperature profiles for one and three PFRs in series for the styrene production process.

lation section to the first reactor (from 17.5 to 14.1 mol/s), resulting in a smaller external compressor (annualised cost of 0.018 M$/yr) and in operational savings (0.02 M$/yr). The reactors in the process with three PFRs in series further require less heating of the reaction section (Table 6) resulting in 0.05 M$/yr cost savings. The temperature profile for both structures is presented in Fig. 7. Due to the cost expression employed, three reactors are more expensive than just one with the same overall catalyst load (Table 5).

The lower cost of the heat exchanger network required for the process with three PFRs can be mainly explained as a combination of two factors. First, there is less recycle from the distillation section to the inlet of the reactor to be heated. Second, there is 36% less water to be fed and therefore to be heated. The overall effect is a 24% reduction of the heat exchange area target. However, the process with three PFRs requires four more heat exchangers as compared to the single PFR structure. Still, the net result is a lower cost heat exchanger network saving 0.037 M$/yr overall.

As a result of the conclusions extracted in the multi-level approach, the proposed optimal conceptual process design candidates for detailed study are the processes with either two or three PFRs (MTRs) in series and ethylbenzene feed distribution (Fig. 8). The design closely approaches the target identified in Level 2A and outperforms a process with a conventional adiabatic reactor by 18% in terms of the profit objective employed.

All optimal solutions for levels 1, 2a and 2b have as an active constraint the lower SOR limit at the inlet of every active reactor, which is specified as seven [29] to prevent coke formation on the catalyst surface and to eliminate coke deposits from the catalyst surface to regenerate it. This explains the preference for solutions in which ethylbenzene feed is distributed in Level 1 and the higher performances of 2 and 3 MTRs with respect to a single one. In addition, the operating temperature in the reactors is limited for all active reactors by the feasible heat exchange media profiles as defined in Fig. 2 at least in one discretisation point. Finally, the maximum amount of catalyst load for each superstructure is also an active constraint for all solutions in all synthesis levels. In terms of reactor choices, MTRs are the main reactor type in the final solutions. This is due to the greater heat exchange areas that these reactor types offer over FBRs and CSTRs.

6. Concluding remarks

A conceptual process design method for heterogeneously catalysed gas-phase reaction systems has been presented. The method is based on tailored process superstructure optimisation schemes and enables the identification of the performance limits of the system as well as the evaluation of the relationship between individual design

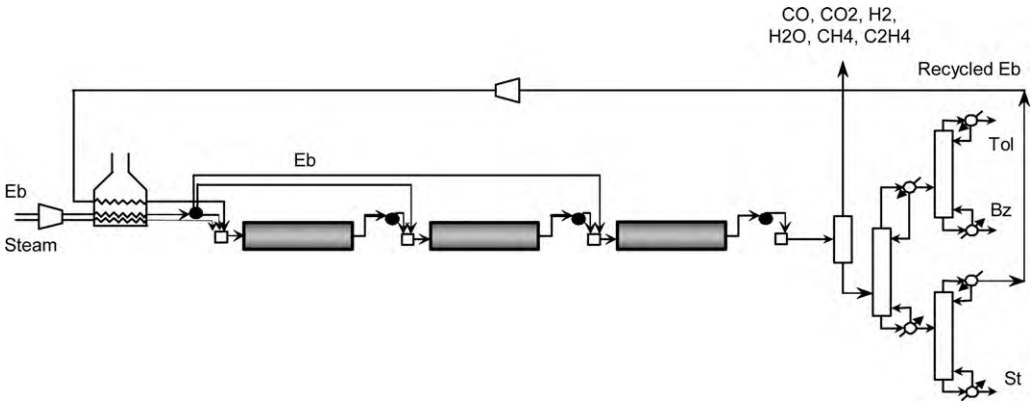

Fig. 8. Conceptual design candidate after Level 2B.

features and performance through a multi-level synthesis strategy. This allows the coordinated exploration of trade-offs between performance and structural complexity.

The method leads to a number of potential design candidates that provide the design engineers with insight into the performance gains that can be expected by increasing design complexity. This information is useful to the design engineers to support decisions on the acceptable trade-off between the level of complexity and the performance. Further, more detailed studies can then be targeted to only a few alternative process designs. Similarly, additional studies can be targeted to explore design trends for changes in economic parameters as the choice of the best solution is often sensitive to differences in feedstock and utility costs of the ranges that are normally seen between different locations. The evolution of the promising designs using detailed models will be the subject of a separate publication.

Appendix A. Modelling information

The overall heat transfer coefficient (U) is determined according to:

$$\frac{1}{U} = \frac{1}{U_{\text{reactive\_media}}} + \frac{\delta_{\text{wall}}}{\lambda_{\text{wall}}} + \frac{1}{U_{\text{utility\_media}}} \tag{A1}$$

where δ_{wall} is the thickness of the wall of the reactor tubes and λ_{wall} its conductivity. The overall heat transfer coefficient for the utility media ($U_{\text{utility\_media}}$) is set to a typical value for its kind. The calculation of the overall heat transfer coefficient for the reactive media ($U_{\text{reactive\_media}}$) depends on the mixing pattern (CSTR or PFR): CSTRs are assumed to have a conical section shape and their overall heat transfer coefficient for the reactive media is assumed to be 600 W/m^2/K for the petrochemical applications studied using the proposed approach. A fluidised bed reactor (FLBR) is a type of reactor that can be represented by a CSTR and has the best heat transfer properties. Since what it is intended to do is to set a maximum limit on the heat exchanged, the heat transfer coefficient for the reactive media has been chosen to be 75% of the highest value for a FLBR found in the literature (Kelkar and Ng [31] suggest values between 50 and 800 W/m^2/K). For PFRs (FBRs or MTRs), the overall heat transfer coefficient for the reactive media is calculated from Dixon [32]:

$$\frac{1}{U_{\text{reactive\_media}}} = \frac{1}{h_{\text{w}}} + \frac{r_{\text{t}}}{3\lambda_{\text{e,r}}}\frac{\text{Bi}+3}{\text{Bi}+4} \tag{A2}$$

Following Koning [33], the wall heat transfer coefficient (h_{w}) can be correlated to the effective radial thermal conductivity ($\lambda_{\text{e,r}}$) of the bed using the Biot number (Bi) and the radius of the tube (r_{t}):

$$\text{Bi} = \frac{h_{\text{w}} r_{\text{t}}}{\lambda_{\text{e,r}}} = 1.5NRe^{-0.25} \tag{A3}$$

where the aspect ratio (N) is:

$$N = \frac{d_{\text{t}}}{d_{\text{p}}} \tag{A4}$$

and d_{t} is the diameter of the tube and d_{p} is the diameter of the catalyst particle. For the cases where the catalyst particles are cylinders, the diameter of the sphere of the catalyst particles is substituted by the equivalent diameter of the sphere of the catalyst particles (d_{p}^{v}):

$$d_{\text{p}}^{\text{v}} = d_{\text{p}}\left(\frac{3}{2}\frac{h_{\text{p}}}{d_{\text{p}}}\right)^{1/3} \tag{A5}$$

where h_{p} is the height of the catalyst particle. Then, the effective radial thermal conductivity can be expressed as the sum of two terms:

$$\lambda_{\text{e,r}} = \lambda_{\text{r}}^{0} + \lambda_{\text{r}}^{\text{f}} \tag{A6}$$

where λ_{r}^{0} is the effective thermal conductivity due to conduction in the fluid and the solid phase and $\lambda_{\text{r}}^{\text{f}}$ is the effective thermal conductivity due to convection. With the help of the fluid conductivity (λ_{f}), the previous equation can be written in dimensionless form as:

$$\frac{\lambda_{\text{e,r}}}{\lambda_{\text{f}}} = \frac{\lambda_{\text{r}}^{0}}{\lambda_{\text{f}}} + \frac{Pe_{\text{h}}^{0}}{Pe_{\text{h,r}}^{\infty}} \tag{A7}$$

where $Pe_{\text{h,r}}$ is the Peclet number for radial heat conduction (∞ indicates at sufficient high velocity) and Pe_{h}^{0} is the fluid Peclet number for heat transfer, which can be expressed as:

$$Pe_{\text{h}}^{0} = \frac{u_0 \rho_{\text{f}} \text{Cp}_{\text{f}} d_{\text{p}}^{\text{v}}}{\lambda_{\text{f}}} = Re \cdot Pr \tag{A8}$$

where u_0 is the superficial velocity, ρ_{f} is the density of the fluid, Cp_{f} is the fluid specific heat and Pr is the Prandtl number. Bauer and Schlünder [34] proposed the following expression for the Peclet number for radial heat conduction:

$$Pe_{\text{h,r}}^{\infty} = 8 \cdot \left[2 - \left(1 - \frac{2}{N}\right)^2\right] \tag{A9}$$

After omitting radiation and direct particle-to-particle heat transfer contributions and the system pressure influence, Bauer and Schlünder [35] found the following expression for the ratio $\lambda_{\text{r}}^{0}/\lambda_{\text{f}}$:

$$\begin{aligned}
&\frac{\lambda_{\text{r}}^{0}}{\lambda_{\text{f}}} = (1 - \sqrt{1-\varepsilon}) + \frac{2\sqrt{1-\varepsilon}}{1 - B\kappa^{-1}}\left[\frac{B(1-\kappa^{-1})}{(1-B\kappa^{-1})^2}\ln\left(\frac{\kappa}{B}\right) - \frac{B-1}{1-B\kappa^{-1}} - \frac{B+1}{2}\right] \\
&B = C_{\text{f}}\left(\frac{1-\varepsilon}{\varepsilon}\right)^{1.11} \qquad C_{\text{f}} = 2.5\left(1 + \left(\frac{d_{\text{i}}}{d_{\text{p}}}\right)\right) \text{ (for rings)} \\
&C_{\text{f}} = 2.5 \text{ (for cylinders)} \quad C_{\text{f}} = 1.25 \text{ (for spheres)}
\end{aligned} \tag{A10}$$

where d_{i} is the inner ring diameter and the ratio of thermal conductivities of the solid and the fluid phase (κ) can be considered to be 10 [36]. The void fraction (ε) for randomly filled beds can be measured following Winterberg and Tsotsas [37] who proposed its calculation as:

$$\begin{aligned}
&\varepsilon(r) = \varepsilon_{\infty}\left(1 + A\exp\left[-B\frac{r_{\text{t}} - r}{d_{\text{p}}}\right]\right) \\
&A = \frac{0.65}{\varepsilon_{\infty}} - 1 \\
&B = 0.6
\end{aligned} \tag{A11}$$

where r accounts for the radial position inside the tube. For dense beds of cylinders with height of particle similar to length of particle, ε_{∞} is in the range between 0.25 and 0.35 [37]. The value selected in this work is $\varepsilon_{\infty} = 0.3$. ∞ Accounts here for an infinitely expanded bed. By integration, the average bed porosity is derived as

$$\bar{\varepsilon} = \frac{2}{r_{\text{t}}}\int_0^{r_{\text{t}}} \varepsilon(r) r \, dr \tag{A12}$$

Appendix B. Problem data for illustrative example

The problem data in terms of prices for the raw materials and products and data related to the reactors are summarised in

Table A1
Problem data.

Parameter	Unit	Value
Ethylbenzene price	$/ton	429.51
Styrene price	$/ton	988.94
Benzene price	$/ton	394.30
Toluene price	$/ton	367.91
Ethylene price	$/ton	0.0
Methane price	$/ton	0.0
Superheated steam price	$/ton	19.98
Max. catalyst load per design Elnashaie et al. [26]	kg	10,895
Wall thickness	m	2×10^{-3}
Thermal conductivity of wall	W/m/K	15
Maximum permissible temperature	K	1000
Minimum permissible temperature	K	400
Catalyst particle height	m	4.7×10^{-3}
Catalyst particle diameter	m	4.7×10^{-3}
Cold utility heat transfer coefficient (molten salt)	W/m^2/K	7523
Hot utility heat transfer coefficient (molten salt)	W/m^2/K	19,873

Table A1. In designs with more than one reactor present, the catalyst load used within the superstructure must remain below the maximum catalyst load. Catalyst particles are assumed to be cylindrical. The molar ratio of the steam to ethylbenzene, SOR (steam over reactant), is required to be greater than seven to prevent coke formation on the catalyst surface and to eliminate coke deposits from the catalyst surface [29]. SOR is restricted to remain below 20 to follow industrial practice [29]. Since styrene catalyst is relatively cheap and is only replaced every 1–2 years [38], its impact on the total cost is very low. Therefore, the catalyst cost is not considered in the objective function. The cost of the FBR is calculated as the cost of a pressure vessel [39]:

$$\mathrm{FBR_{cost}} = F_{\mathrm{P}}(10^{K1+K2\cdot\log(\mathrm{volume_{reactor}})} + K3\cdot\log(\mathrm{volume^2_{reactor}})) \quad \text{(B1)}$$

where:

$$F_{\mathrm{p}} = \frac{(P_{\max}+1.0)D_{\mathrm{v}}}{[[2.0(850-0.6(P_{\max}+1))]+0.00315]\cdot 0.0063} \quad \text{(B2)}$$

where D_{v} is the diameter of the vessel and $P_{\max}$ the maximum pressure in the vessel. The parameters take the following values: $K_1 = 3.49$, $K_2 = 0.38$ and $K_3 = 0.09$. CSTR and MTRs are priced multiplying a factor (5 and 30, respectively) by the price of a FBR with the same catalyst load. The factors are derived from information obtained from ASPEN Icarus and Luyben [40].

Short-cut distillation methods are employed to model the distillation columns. It is assumed that this case study is a retrofit scenario in terms of reactors, in which the separation section is already in place when the synthesis exercise begins. The equations employed are the Fenske equation to calculate Nmin, the Underwood algorithm to calculate Rmin and the Gilliland correlation in the Eduljee form to calculate the reflux. The condensed fractions in the condenser are assumed to be 100%, 99.5%, 99% and 98% for styrene, ethylbenzene, toluene and benzene respectively [41]. The exit temperature of the cooler prior to the flash unit is set at 333 K at a pressure of 1.9 bar. The solubility of non-condensable gases in the organic phase is assumed to be negligible, and the organic compounds totally immiscible in water. In the first distillation column after the flash drum, the recovery fractions for the light key component (toluene) and for the heavy key component (ethylbenzene) are assumed to be 99.9%. In the benzene/toluene distillation column, the recovery fraction for toluene is assumed at 99.9% with a purity of 99.7%. In the ethylbenzene/styrene distillation column, the recovery fraction for styrene is assumed at 99.7% with a purity of 99.7%. The amount of ethylbenzene recovered in the column and recycled to the first reactor is calculated by short-cut design method. Since the fraction recovered in the column must be specified in advance to close the recycle, the recovery for ethylbenzene fed to the column is assumed to be 99.9%. The structure is accepted if the calculated and estimated values are within a specified tolerance according to:

$$-0.001 \le \frac{\mathrm{fraction\_calculated} - 0.999}{0.999} \le 0.001 \quad \text{(B3)}$$

For all the distillation columns the reflux is assumed to be 1.1 times the minimum reflux. All streams into and out of the columns are considered for the heat integration.

The cold utility is specified to be cooling water that is fed to the system at 300 K and returned at 319 K with a cost of 2.47×10^{-7} $/gmol [42]. The process heating requirements are met by a hot utility and by a furnace. The price of the hot utility is assumed at $60/kWyr. The price of furnace fuel is 174 $/kWyr [43]. Reactors are not heat integrated with the rest of the process because of controllability issues. If the reactor requires heating, a cost of 174 $/kWyr is applied. The capital cost for the heat exchanger network is estimated according to Luyben [40] assuming heat exchangers with equal area [44]. The fixed cost of the furnace is estimated according to Tantimuratha et al. [43]. The compressors are assumed to perform adiabatic compression of ideal gases with 75% efficiency and are costed according to [40]. The price of electricity is assumed at $0.07 kWh. The interest rate is set to 5% and the payback period to 3 years.

References

[1] A.C. Kokossis, C.A. Floudas, Optimisation of complex reactor networks – I. Isothermal operation, Chemical Engineering Science 45 (3) (1990) 595–614.
[2] A.C. Kokossis, C.A. Floudas, Synthesis of isothermal reactor–separator-recycle systems, Chemical Engineering Science 46 (5–6) (1991) 1361–1383.
[3] E.C. Marcoulaki, A.C. Kokossis, Scoping and screening complex reaction networks using stochastic optimisation, AIChE Journal 45 (9) (1999) 1977–1991.
[4] W. Rooney, B.P. Hausberger, L.T. Biegler, D. Glasser, Convex attainable region projections for reactor network synthesis, Computers & Chemical Engineering 24 (2–7) (2000) 225–229.
[5] W.R. Esposito, C.A. Floudas, Deterministic global optimization in isothermal reactor network synthesis, Journal of Global Optimization 22 (2002) 59–95.
[6] V.M. Ashley, P. Linke, A novel approach to reactor network synthesis using knowledge discovery and optimisation techniques, Chemical Engineering Research & Design 82 (8) (2004) 952–960.
[7] A. Posada, V. Manousiouthakis, Multi-feed attainable region construction using the Shrink–Wrap algorithm, Chemical Engineering Science 63 (2008) 5571–5592.
[8] E.C. Marcoulaki, P. Linke, A.C. Kokossis, Design of separation trains and reaction–separation networks using stochastic optimization methods, Chemical Engineering Research & Design 79 (A1) (2001) 25–32.
[9] S.R. Ismail, P. Proios, E.N. Pistikopoulos, Modular synthesis framework for combined separation/reaction systems, AIChE Journal 47 (2001) 629–649.
[10] P. Linke, A.C. Kokossis, Attainable designs for reaction and separation processes from a superstructure-based approach, AIChE Journal 49 (6) (2003) 1451–1470.
[11] P. Linke, A.C. Kokossis, A multi-level methodology for conceptual reaction–separation process design, Chemical Product and Process Modelling 2 (3) (2007) 2, Article.
[12] P. Linke, A.C. Kokossis, On the robust application of stochastic optimisation technology for the synthesis of reaction/separation systems, Computers & Chemical Engineering 27 (5) (2003) 733–758.
[13] S. Rigopoulos, P. Linke, Systematic development of optimal activated sludge process designs, Computers & Chemical Engineering 26 (4–5) (2002) 585–597.
[14] A.I. Papadopoulos, P. Linke, Integrated solvent and process selection for separation and reactive separation systems, Chemical Engineering and Processing: Process Intensification 48 (2009) 1047–1060.
[15] P. Linke, A.C. Kokossis, Advanced process design technology for pollution prevention and waste treatment, Advances in Environmental Research 8 (2) (2004) 229–245.
[16] D. Montolio-Rodriguez, D. Linke, P. Linke, Systematic identification of optimal process designs for the production of acetic acid via ethane oxidation, Chemical Engineering Science 62 (2007) 5602–5608.
[17] S.W. Hwang, P. Linke, R. Smith, Heterogeneous catalytic reactor design with optimum temperature profile II: application of non-uniform catalyst, Chemical Engineering Science 59 (20) (2004) 4245–4260.
[18] S. Ergun, Fluid flow through packed columns, Chemical Engineering Progress 48 (2) (1952) 89–94.
[19] B. Linnhoff, J.R. Flower, Synthesis of heat exchanger networks: I. Systematic generation of energy optimal networks, AIChE Journal 24 (4) (1978) 633–642.
[20] D.W. Townsend, B. Linnhoff, Surface area targets for heat exchanger networks, in: IChemE 11th Annual Research Meeting on Heat Transfer, Bath, 1984.
[21] B. Linnhoff, D.R. Mason, I. Wardle, Understanding heat exchanger networks, Computes & Chemical Engineering 3 (1–4) (1979) 295–302.
[22] F. Glover, Future paths for integer programming and links to artificial intelligence, Computers and Operations Research 13 (5) (1986) 533–549.

[23] B. Lin, D.C. Miller, Tabu search algorithm for chemical process optimization, Computers & Chemical Engineering 28 (11) (2004) 2287–2306.
[24] L. Cavin, U. Fischer, F. Glover, K. Hungerbuhler, Multi-objective process design in multi-purpose batch plants using a Tabu Search optimisation algorithm, Computers & Chemical Engineering 28 (4) (2004) 459–478.
[25] H.S. Chen, M.A. Stadtherr, A modification of Powell's Dogleg method for solving systems of non-linear equations, Computers & Chemical Engineering 5 (3) (1981) 143–150.
[26] S.S.E.H. Elnashaie, B.K. Abdallah, S.S. Elshishini, S. Alkhowaiter, M.B. Noureldeen, T. Alsoudani, On the link between intrinsic catalytic reactions kinetics and the development of catalytic process. Catalytic dehydrogenation of ethylbenzene to styrene, Catalysis Today 64 (3–4) (2001) 151–162.
[27] B.K. Abdalla, S.S.E.H. Elnashaie, S. Alkhowaiter, E. Elshishini, Intrinsic kinetics and industrial reactors modeling for the dehydrogenation of ethylbenzene to styrene on promoted iron oxide catalysts, Applied Catalysis A: General 113 (1994) 89–102.
[28] S.S.E.H. Elnashaie, S.S. Elshishini, Modelling, Simulation and Optimization of Industrial Fixed Bed Catalytic Reactors, Gordon and Breach Science Publisher, London, 1994.
[29] A.K.Y. Yee, A.K. Ray, G.P. Rangaiah, Multi-objective optimizations of an industrial styrene reactor, Computers & Chemical Engineering 27 (1) (2003) 111–130.
[30] J.G.P. Sheel, C.M. Crowe, Simulation and optimization of an existing ethyl benzene dehydrogenation reactor, Canadian Journal of Chemical Engineering 47 (1969) 183–187.
[31] V.V. Kelkar, K.M. Ng, Screening multi-phase reactors for non-isothermal multiple reactions, AIChE Journal 46 (2) (2000) 389–406.
[32] A.G. Dixon, An improved equation for the overall heat transfer coefficient in packed beds, Chemical Engineering and Processing 35 (5) (1996) 323–331.
[33] B. Koning, Heat and mass transport in tubular packed bed reactors at reacting and non-reacting conditions, Ph.D. Thesis, University of Twente, 2002.
[34] R. Bauer, E.U. Schlünder, Effective radial thermal conductivity of packings in gas flow. Part I. Convective transport coefficient, International Chemical Engineering 18 (1978) 181–189.
[35] R. Bauer, E.U. Schlünder, Effective radial thermal conductivity of packings in gas flow. Part II. Thermal conductivity of the packing fraction without gas flow, International Chemical Engineering 18 (1978) 189–204.
[36] E.I. Smirnov, V.A. Kuzmin, I.A. Zolotarskii, Radial thermal conductivity in cylindrical beds packed by shaped particles, Chemical Engineering Research and Design 82 (A2) (2004) 293–296.
[37] M. Winterberg, E. Tsotsas, Correlations for effective heat transport coefficients in beds packed with cylindrical particles, Chemical Engineering Science 55 (23) (2000) 5937–5943.
[38] G.R. Meima, P.G. Menon, Catalyst deactivation phenomena in styrene production, Applied Catalysis A: General 212 (1–2) (2001) 239–245.
[39] R. Turton, Personal communication, 2005.
[40] W.L. Luyben, Design of cooled tubular reactor systems, Industrial Engineering and Chemistry Research 40 (24) (2001) 5775–5783.
[41] A. Tarafder, G.P. Rangaiah, A.K. Ray, Multi-objective optimization of an industrial styrene monomer manufacturing process, Chemical Engineering Science 60 (2) (2005) 347–363.
[42] L.T. Biegler, I.E. Grossmann, A.W. Westerberg, Systematic Methods of Chemical Process Design, Prentice-Hall, Englewood Cliffs, NJ, 1997.
[43] L. Tantimuratha, A.C. Kokossis, F.U. Muller, The heat exchanger network design as a paradigm of technology integration, Applied Thermal Engineering 20 (15–16) (2000) 1589–1605.
[44] S. Ahmad, B. Linnhoff, R. Smith, Cost optimum heat exchanger networks – 2. Targets and design for detailed capital cost models, Computers & Chemical Engineering 14 (7) (1990) 751–767.